

Solar PV Array-Fed Water Pumping System Using Zeta Converter based Closed-Loop Control of BLDC Motor Drive

R. Durgaprasad

Department of Electrical &
Electronics Engineering,
AITAM, Srkakulam, India.

P. Guruvulunaidu

Department of Electrical &
Electronics Engineering,
AITAM, Srikakulam, India.

Ch. Prasad

Department of Electrical &
Electronics Engineering,
AITAM, Srikakulam, India.

Abstract: This paper proposes a solar photovoltaic (SPV) array fed water pumping system utilizing a zeta converter as an intermediate DC-DC converter in order to extract the maximum available power from the SPV array. Controlling the zeta converter in an intelligent manner through the incremental conductance maximum power point tracking (INC-MPPT) algorithm offers the soft starting of the brushless DC (BLDC) motor employed to drive a centrifugal water pump coupled to its shaft. Soft starting i.e. the reduced current starting inhibits the harmful effect of the high starting current on the windings of the BLDC motor. A fundamental frequency switching of the voltage source inverter (VSI) is accomplished by the electronic commutation of the BLDC motor, thereby avoiding the VSI losses occurred owing to the high frequency switching. A new design approach for the low valued DC link capacitor of VSI is proposed. The proposed water pumping system is designed and modeled such that the performance is not affected even under the dynamic conditions. Suitability of the proposed system under dynamic conditions is demonstrated by the simulation results using MATLAB/Simulink software.

Key words: Brushless dc (BLDC) motor, incremental conductance maximum power point tracking (INC-MPPT), solar photovoltaic (SPV) array, voltage-source inverter (VSI), water pump, zeta converter

I.INTRODUCTION

Severe environmental protection regulations, shortage of fossil fuels and eternal energy from the sun have motivated the researchers towards the solar photovoltaic (SPV) array generated electrical power for various applications [1]. Water pumping is receiving wide attention now a days amongst all the applications of SPV array. To enhance the efficiency of SPV array and hence the whole system regardless of the operating conditions, it becomes essential to operate SPV array at its maximum power point by means of a maximum power point tracking (MPPT) algorithm [2-4]. Various DC-DC converters have been already employed to accomplish this action of MPPT. Nevertheless, a Zeta converter [5-9] based MPPT is still unexplored in any kind of SPV array based applications. An incremental conductance (INC) MPPT algorithm [2] is used in this work in order to generate an optimum value of duty cycle for the IGBT (Insulated Gate Bipolar Transistor) switch of Zeta converter such that the SPV array is constrained to operate at its MPP. Various configuration of

Zeta converters such as self-lift circuit, re-lift circuit, triple-lift circuit and quadruple-lift circuit using voltage lift (VL) technique have been reported in aforementioned topologies have high voltage transfer gain but at the cost of increased number of components and switching devices. Therefore, these topologies of Zeta converter do not suit the proposed water pumping system.

The PV inverters dedicated to the small PV plants must be characterized by a large range for the input voltage in order to accept different configurations of the PV field. This capability is assured by adopting inverters based on a double stage architecture where the first stage, which usually is a dc/dc converter, can be used to adapt the PV array voltage in order to meet the requirements of the dc/ac second stage, which is used to supply an ac load or to inject the produced power into the grid. This configuration is effective also in terms of controllability because the first stage can be devoted to track the maximum power from the PV array, while the second stage is used to produce ac current with low Total Harmonic Distortion (THD).

BLDC motors are preferred over DC motors and induction motors due to their advantages like long operating life, higher efficiency, low maintenance and better speed torque characteristics. Stator windings of BLDC motors are energized in a sequence from an inverter. A bulkier DC link capacitor is connected in between the dc-dc converter and inverter to get a constant voltage at the input of inverter, thus to make the voltage ripple free. But the DC link capacitor is bulkier in size and its life time is affected by operating temperature. Moreover the cost is about 5-15% of overall cost of BLDC motor drive. As an attempt to reduce the cost of motor, DC link capacitor can be eliminated at the expense of torque ripple. Thus a new torque ripple compensation technique is proposed to compensate for the torque ripple associated with the elimination of the DC link capacitor. In this method, torque ripple compensation technique is proposed to a solar PV array fed DC link capacitor free BLDC motor.

The permanent magnet brushless DC (BLDC) motor is employed to drive a centrifugal water pump coupled to its shaft. The BLDC motor is selected because of its merits [7,9] useful for the development of suitable water pumping system. This electronically commutated BLDC motor [9-11] is supplied by a voltage source inverter (VSI) which is operated by fundamental frequency switching resulting in

low switching losses [12-15]. Suitability of the proposed SPV array fed water pumping system subjected to various operating and environmental conditions is demonstrated by satisfactory simulated results using MATLAB/Simulink environment.

The existing literature exploring SPV array-based BLDC motor-driven water pump is based on a configuration shown in Fig.1. A dc-dc converter is used for MPPT of an SPV array as usual. Two phase currents are sensed along with Hall signals feedback for control of BLDC motor, resulting in an increased cost. The additional control scheme causes increased cost and complexity, which is required to control the speed of BLDC motor. Moreover, usually a voltage-source inverter (VSI) is operated with high-frequency PWM pulses, resulting in an increased switching loss and hence the reduced efficiency.

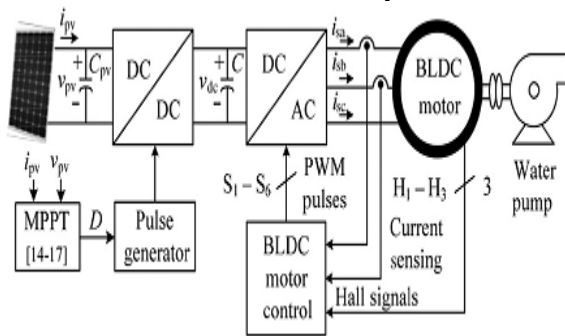


Fig.1. Conventional SPV-fed BLDC motor-driven water pumping system

II. PV PANEL MODELING

Equivalent circuit model of a PV string is indicated in fig. 2(a). In this model, I_{sc} is the generated current of a PV string and R_s and R_p are the series and parallel resistances of a string. Also, equivalent circuit model of multiple strings are shown in fig. 2(b). In this figure, bypass diode is considered for each string. To obtain the V-I characteristic of a PV, below equation is used:

$$I = I_{sc} - I_0 \left(e^{\frac{q(v+R_s I)}{kT}} - 1 \right) - \left(\frac{v + R_s I}{R_p} \right)$$

Where T, q, k and I_0 are the temperature (K), the electron charge (C), $q=1.602 \times 10^{-19}$ C, Boltzmann's constant ($k=1.381 \times 10^{-23}$ J/K) and the reverse saturation current (A), respectively. In a PV panel, the generated maximum power is the point that the product ($V \times I$) is maximum which is called maximum power point (MPP). It is obvious that the irradiation and temperature are two important factors in the value of generated electricity by a PV panel which affect the point of generated maximum power.

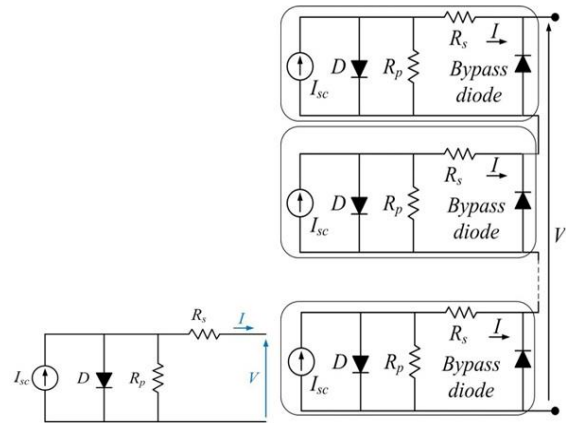


Fig.2. Equivalent circuit model of (a) a PV string model, (b) multiple PV strings model.

III. ZETA CONVERTER

The proposed converter is based on DC-DC converter to maintain the constant output voltage. The sixth DC-DC converter that we will study now was developed at the end of the 1980s, separately by Kazimierzczuk, under the name of Dual SEPIC, and Barbi, under the name of Zeta converter (from the sixth letter of the Greek alphabet, to correspond to the "sixth" converter). Zeta is a fourth order DC-DC converter. Zeta converter will vary above or below the input voltage without change in output polarity. A Zeta is similar to a BUCK – BOOST converter but has advantages of having non-inverted output (the output voltage is of the same polarity as the input voltage). The inductors and the capacitors can also have large effects on the converter efficiency and ripple voltage. This converter transfers the energy between the inductance and the capacitance in order to change from the voltage to another. The transferred energy is controlled by switching device S (MOSFET).

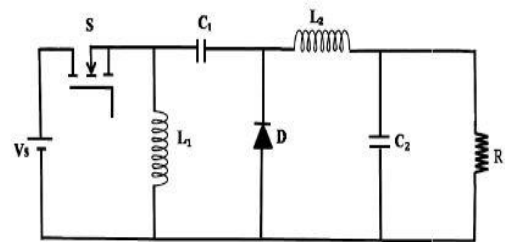


Fig.3. Schematic Diagram of Zeta Converter

A. Operating Modes Of Zeta Converter

The converter circuit is divided into two parts as shown in fig.4 and fig.5. In mode 1 the switch will be closed as shown in fig.4. When S is turning on (ON-state), the diode is off. This is shown as an open circuit (for diode) and short circuit (for S). In this time interval diode D1 is OFF with a reverse voltage equal to $-(V_s + V_o)$. During this state, inductor L_1 and L_2 are in charge phase. These mean that the inductor current i_{L1} and i_{L2} increase linearly.

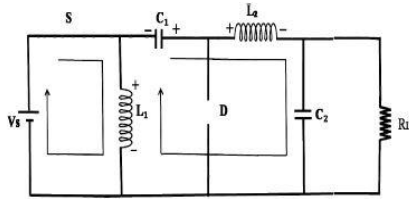


Fig.4.Zeta Converter when switch is ON

The capacitor C₁ will discharge and the energy will be charged to V₀ and it is connected in series with L₂. The sum of the charging inductor current flows through S.

Applying the Kirchhoff's voltage law to the circuit in Fig.4 and writing the voltage equations

$$\frac{di_{L1}}{dt} = \frac{V_s}{L_1}$$

$$\frac{di_{L2}}{dt} = \frac{V_s}{L_2} + \frac{V_{C1}}{L_2} - \frac{V_{C2}}{L_2}$$

By applying Kirchhoff's current law the rate of voltage through the capacitors will be,

$$\frac{dV_{C1}}{dt} = -\frac{i_{L2}}{C_1}$$

$$\frac{dV_{C2}}{dt} = \frac{i_{L2}}{C_2} - \frac{V_{C2}}{R_L C_2}$$

In mode 2 the switch will be open as shown in fig.4. When S is turning off (OFF-state), the diode is on. Opposite to previous ON-state, the equivalent circuit shows that the diode is short circuit and S is open circuit. Inductor L₁, that was previously charged will now have to be in a discharging. At this state, inductor L₁ and L₂ are in discharge phase. Since the voltage polarity of the inductor changes the diode will get forward biased and it will conduct.

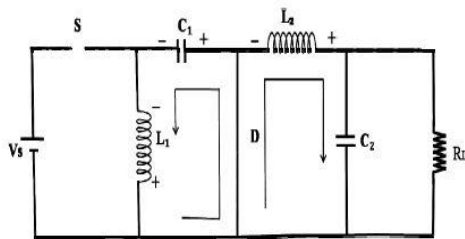


Fig.5. Zeta Converter when switch is OFF

Energy in L₁ and L₂ are discharged to capacitor C₁ and output part, respectively. As a result, inductor current i_{L1} and i_{L2} are decreasing linearly.

By applying Kirchhoff's voltage law, voltage across inductor L₁ is expressed as,

$$\frac{di_{L1}}{dt} = -\frac{V_{C1}}{L_1}$$

$$\frac{di_{L2}}{dt} = -\frac{V_{C2}}{L_2}$$

By applying Kirchhoff's current law, current flows through the capacitor C₁ is expressed as,

$$\frac{dV_{C1}}{dt} = \frac{i_{L1}}{C_1}$$

The relation between input and output voltages of the zeta converter is given by

The duty cycle D for zeta converter in CCM is given by,

$$D = \frac{V_0}{V_0 + V_s}$$

$$\frac{D}{(1-D)} = \frac{V_0}{V_s} = \frac{i_s}{i_0}$$

IV. PRINCIPLE OF BLDC MOTOR

A three-phase brushless DC motor has three induction coils with equivalent circuit of BLDC motors as described in the following section.

A. Mathematical Model of the BLDC Motor:

The equivalent circuit of BLDC motor is shown in Fig.6. The dynamic equations of BLDC motor may be expressed in matrix form:

$$\begin{bmatrix} V_a \\ V_b \\ V_c \end{bmatrix} = R \begin{bmatrix} 1 & 0 & 0 \\ 0 & 1 & 0 \\ 0 & 0 & 1 \end{bmatrix} \begin{bmatrix} I_a \\ I_b \\ I_c \end{bmatrix} + \begin{bmatrix} L-M & 0 & 0 \\ 0 & L-M & 0 \\ 0 & 0 & L-M \end{bmatrix} \frac{d}{dt} \begin{bmatrix} I_a \\ I_b \\ I_c \end{bmatrix} + \begin{bmatrix} E_a \\ E_b \\ E_c \end{bmatrix}$$

The electromagnetic torque developed by the motor is given by

$$T_e = \frac{E_a I_a + E_b I_b + E_c I_c}{\omega}$$

The moment of inertia includes all inertia connected to the motor shaft, and damping constant includes the air friction and the bearing friction. Therefore, the torque equation is

$$J \frac{d\omega}{dt} + B\omega = T_e - T_l$$

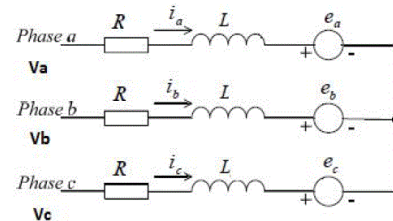


Fig.6. The Equivalent Circuit Of BLDC Motor

A. The BLDC Motor Control:

BLDC motors are driven by a three-phase inverter with six-step commutation sequence. The inverter is commutated every 60 degree electrical when H_a, H_b and H_c are Hall effect sensor signal of each phase as shown in Fig.7.

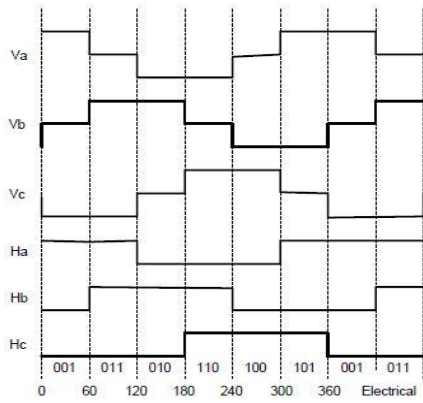


Fig.7. Six Step Commutation Sequence

B. BLDC Motor's Back EMF:

The 2 coils are induced to rotate through a magnetic field; the induced voltage is created in this coils, call that "Back Electromotive force" or "Back-EMF". The relation between Back-EMF signal and Hall effect sensor of each phase is shown in Fig.8.

V.CONFIGURATION OF PROPOSED SYSTEM

The structure of proposed SPV array-fed BLDC motor driven water pumping system employing a zeta converter is shown in Fig.9. The proposed system consists of (left to right) an SPV array, a zeta converter, a VSI, a BLDC motor, and a water pump. The BLDC motor has an inbuilt encoder. The pulse generator is used to operate the zeta converter. A step-by-step operation of proposed system is elaborated in Section III in detail.

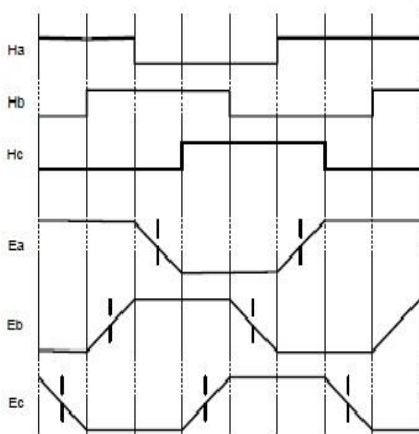


Fig.8. Back EMF signal and Hall Effect sensor

VI. OPERATION OF PROPOSEDSYSTEM

The SPV array generates the electrical power demanded by the motor-pump. This electrical power is fed to the motor pump via a zeta converter and a VSI. The SPV array appears as a power source for the zeta converter as shown in Fig.9. Ideally, the same amount of power is transferred at the output of zeta converter which appears as an input source for the VSI. In practice, due to the various losses associated with a dc-dc converter, slightly less amount of power is transferred to feed the VSI. The pulse generator generates, through INCMPPPT algorithm, switching pulses for insulated

gate bipolar transistor (IGBT) switch of the zeta converter. The INC-MPPT algorithm uses voltage and current as feedback from SPV array and generates an optimum value of duty cycle. Further, it generates actual switching pulse by comparing the duty cycle with a high-frequency carrier wave. In this way, the maximum power extraction and hence the efficiency optimization of the SPV array is accomplished.

The VSI, converting dc output from a zeta converter into ac, feeds the BLDC motor to drive a water pump coupled to its shaft. The VSI is operated in fundamental frequency switching through an electronic commutation of BLDC motor assisted by its built-in encoder. The high frequency switching losses are thereby eliminated, contributing in an increased efficiency of proposed water pumping system.

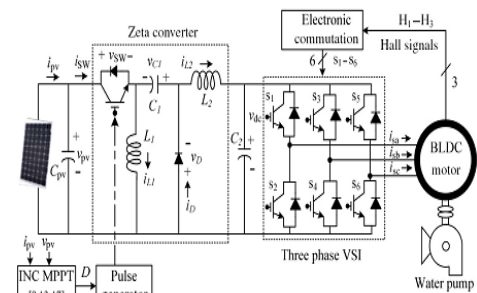


Fig.9. Proposed SPV-zeta converter-fed BLDC motor drive for water pump

VII. DESIGN OF PROPOSEDSYSTEM

Various operating stages shown in Fig.9 are properly designed to develop an effective water pumping system, capable of operating under uncertain conditions. A BLDC motor of 2.89-kW power rating and an SPV array of 3.4-kW peak power capacity under standard test conditions (STC) are selected to design the proposed system. The detailed designs of various stages such as SPV array, zeta converter, and water pump are described as follows.

A. Design of SPV Array

As per above discussion, the practical converters are associated with various power losses. In addition, the performance of BLDC motor-pump is influenced by associated mechanical and electrical losses. To compensate these losses, the size of SPV array is selected with slightly more peak power capacity to ensure the satisfactory operation regardless of power losses. Therefore, the SPV array of peak power capacity of $P_{mpp}=3.4$ kW under STC (STC: 1000 W/m², 25°C, AM 1.5), slightly more than demanded by the motor-pump is selected and its parameters are designed accordingly. Solar World make Sun module Plus SW 280 mono SPV module is selected to design the SPV array of an appropriate size. Electrical specifications of this module are listed in Table1 and numbers of modules required to connect in series/parallel are estimated by selecting the voltage of SPV array at MPP under STC as $V_{mpp}=187.2V$.

TABLE I
 Specifications of Sun module plus SW 280mono SPV Module

Peak power, P_m (W)	280
Open circuit voltage, V_o (V)	39.5
Voltage at MPP, V_m (V)	31.2
Short circuit current, I_s (A)	9.71
Current at MPP, I_m (A)	9.07
Number of cells connected in series, N_{ss}	60

The current of SPV array at MPP I_{mpp} is estimated as

$$I_{mpp} = \frac{P_{mpp}}{V_{mpp}} = \frac{3400}{187.2} = 18.16A$$

The numbers of modules required to connect in series are as follows:

$$N_s = \frac{V_{mpp}}{V_m} = \frac{187.2}{31.2} = 6$$

The numbers of modules required to connect in parallel are as follows:

$$N_p = \frac{I_{mpp}}{I_m} = \frac{18.16}{9.07} = 2$$

Connecting six modules in series, having two strings in parallel, an SPV array of required size is designed for the proposed system.

B. Design of Zeta Converter

To achieve the high performance and efficiency of the dc-dc converter the values of passive elements (Inductor and Capacitor) have significant impact. Here designing equations are used to design zeta converter.

Zeta converter designing equations are as follows:

$$D = \frac{V_{dc}}{V_{mpp} + V_{dc}} = \frac{200}{200 + 187.2} = 0.52$$

$$L_1 = \frac{DV_{mpp}}{f_{sw}\Delta I_{L1}} = \frac{0.52 \times 187.2}{20000 \times 18.16 \times 0.06} \approx 5mH$$

$$L_2 = \frac{(1-D)V_{dc}}{f_{sw}\Delta I_{L2}} = \frac{(1-0.52) \times 200}{20000 \times 17 \times 0.06} \approx 5mH$$

$$C_1 = \frac{DI_{dc}}{f_{sw}\Delta V_{C1}} = \frac{0.52 \times 17}{20000 \times 200 \times 0.1} = 22\mu F$$

Where f_{sw} is the switching frequency of IGBT switch of the zeta converter; ΔI_{L1} is the amount of permitted ripple in the current flowing through L_1 , same as $I_{L1} = I_{mpp}$; ΔI_{L2} is the amount of permitted ripple in the current flowing through L_2 , same as $I_{L2} = I_{dc}$; ΔV_{C1} is permitted ripple in the voltage across C_1 , same as $V_{C1} = V_{dc}$.

C. Estimation of DC-Link Capacitor of VSI

The fundamental output frequency of VSI corresponding to the rated speed of BLDC motor ω_{rated} is estimated as

$$\omega_{rated} = 2\pi f_{rated} = 2\pi \frac{N_{rated}P}{120} = 2\pi \times \frac{3000 \times 6}{120} = 942rad/s$$

The fundamental output frequency of the VSI corresponding to the minimum speed of the BLDC motor essentially required to pump the water ($N = 1100r/min$) ω_{min} is estimated as

$$\omega_{min} = 2\pi f_{min} = 2\pi \frac{NP}{120} = 2\pi \times \frac{1100 \times 6}{120} = 345.57rad/s$$

Where f_{rated} and f_{min} are fundamental frequencies of output voltage of VSI corresponding to a rated speed and a minimum speed of BLDC motor essentially required to pump the water, respectively, in Hz; N_{rated} is rated speed of the BLDC motor; P is a number of poles in the BLDC motor.

The value of dc link capacitor of VSI at ω_{rated} is as follows:

$$C_{2,rated} = \frac{I_{dc}}{6 \times \omega_{rated} \times \Delta V_{dc}} = \frac{17}{6 \times 942 \times 200 \times 0.1} = 150.4\mu F$$

Similarly, a value of dc link capacitor of VSI at ω_{min} is as follows:

$$C_{2,min} = \frac{I_{dc}}{6 \times \omega_{min} \times \Delta V_{dc}} = \frac{17}{6 \times 345.57 \times 200 \times 0.1} = 410\mu F$$

Where ΔV_{dc} is an amount of permitted ripple in voltage across dc-link capacitor C_2 . Finally, $C_2 = 410\mu F$ is selected to design the dc-link capacitor.

D. Design of Water Pump

To estimate the proportionality constant K for the selected water pump, its power-speed characteristics is used as

$$K = \frac{P}{\omega_r^3} = \frac{2.89 \times 10^3}{\left(2\pi \times \frac{3000}{60}\right)^3} = 9.32 \times 10^{-5}$$

Where $P = 2.89$ kW is rated power developed by the BLDC motor and ω_r is rated mechanical speed of the rotor (3000r/min) in rad/s.

A water pump with these data is selected for proposed system.

VIII. CONTROL OF PROPOSED SYSTEM

The proposed system is controlled in two stages. These two control techniques, viz., MPPT and electronic commutation, are discussed as follows.

A. INC-MPPT Algorithm

An efficient and commonly used INC-MPPT technique [8],[13] in various SPV array based applications is utilized in order to optimize the power available from a SPV array and to facilitate a soft starting of BLDC motor. This technique allows perturbation in either the SPV array voltage or the duty cycle. The former calls for a proportional integral (PI) controller to generate a duty cycle [8] for the zeta converter, which increases the complexity. Hence, the direct duty cycle control is adapted in this work. The INC-

MPPT algorithm determines the direction of perturbation based on the slope of $P_{pv}-V_{pv}$ curve, shown in Fig.10. As shown in Fig.10, the slope is zero at MPP, positive on the left, and negative on the right of MPP, i.e.,

$$\begin{aligned} \frac{dP_{pv}}{dv_{pv}} &= 0; \text{ at mpp} \\ \frac{dP_{pv}}{dv_{pv}} &> 0; \text{ left of mpp} \\ \frac{dP_{pv}}{dv_{pv}} &< 0; \text{ right of mpp} \end{aligned}$$

Since

$$\frac{dP_{pv}}{dv_{pv}} = \frac{d(v_{pv} \times i_{pv})}{dv_{pv}} = i_{pv} + v_{pv} \times \frac{di_{pv}}{dv_{pv}} \cong i_{pv} + v_{pv} \times \frac{\Delta i_{pv}}{\Delta v_{pv}}$$

Therefore, (14) is rewritten as

$$\begin{aligned} \frac{\Delta i_{pv}}{\Delta v_{pv}} &= -\frac{i_{pv}}{v_{pv}}; \text{ at mpp} \\ \frac{\Delta i_{pv}}{\Delta v_{pv}} &< -\frac{i_{pv}}{v_{pv}}; \text{ left of mpp} \\ \frac{\Delta i_{pv}}{\Delta v_{pv}} &> -\frac{i_{pv}}{v_{pv}}; \text{ right of mpp} \end{aligned}$$

Thus, based on the relation between INC and instantaneous conductance, the controller decides the direction of perturbation as shown in Fig.10, and increases/decreases the duty cycle accordingly. For instance, on the right of MPP, the duty cycle is increased with a fixed perturbation size until the direction reverses. Ideally, the perturbation stops once the operating point reaches the MPP. However, in practice, operating point oscillates around the MPP.

As the perturbation size reduces, the controller takes more time to track the MPP of SPV array. An intellectual agreement between the tracking time and the perturbation size is held to fulfill the objectives of MPPT and soft starting of BLDC motor. In order to achieve soft starting, the initial value of duty cycle is set as zero. In addition, an optimum value of perturbation size ($\Delta D=0.001$) is selected, which contributes to soft starting and also minimizes oscillations around the MPP.

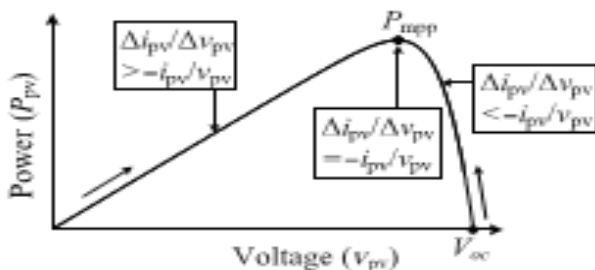


Fig.10. Illustration of INC-MPPT with SPV array $P_{pv}-V_{pv}$ characteristics.

B. Electronic Commutation of BLDC Motor

The BLDC motor is controlled using a VSI operated through an electronic commutation of BLDC motor. An electronic commutation of BLDC motor stands for

commutating the currents flowing through its windings in a predefined sequence using decoder logic. It symmetrically places the dc input current at the center of each phase voltage for 120°. Six switching pulses are generated as per the various possible combinations of three Hall-effect signals. These three Hall-effect signals are produced by an inbuilt encoder according to the rotor position.

TABLE.2
 Switching States for Electronic Commutation of BLDC Motor

Rotor Position $\theta(^{\circ})$	Hall Signals			Switching States					
	H ₃	H ₂	H ₁	S ₁	S ₂	S ₃	S ₄	S ₅	S ₆
NA	0	0	0	0	0	0	0	0	0
0-60	1	0	1	1	0	0	1	0	0
60-120	0	0	1	1	0	0	0	0	1
120-180	0	1	1	0	0	1	0	0	1
180-240	0	1	0	0	1	1	0	0	0
240-300	1	1	0	0	1	0	0	1	0
300-360	1	0	0	0	0	0	1	1	0
NA	1	1	1	0	0	0	0	0	0

A particular combination of Hall-effect signals is produced for each specific range of rotor position at an interval of 60° [5],[6]. The generation of six switching states with the estimation of rotor position is tabularized in Table II. It is perceptible that only two switches conduct at a time, resulting in 120° conduction mode of operation of VSI and hence the reduced conduction losses. Besides this, the electronic commutation provides fundamental frequency switching of the VSI; hence, losses associated with high-frequency PWM switching are eliminated. A motor power company makes BLDC motor with inbuilt encoder is selected for proposed system and its detailed specifications are given in the Appendixes.

IX. CLOSED LOOP SPEED CONTROL OF BLDC MOTOR

In the sensed BLDC drive, hall sensors or a shaft encoder is used to obtain the rotor position information. The drive control system consists of an outer speed loop for speed control and an inner current loop for current control. Conventionally three separate current sensors are used to measure the phase currents. But here only one current sensor is used, which is placed on the DC link.

A. Speed control

The speed control block uses a Proportional Integral (PI) controller. A PI controller attempts to correct the error between a measured process variable and desired set point by calculating and then outputting a corrective action that can adjust the process accordingly. The PI controller calculation involves two separate modes the proportional mode and the integral mode. The proportional mode determine the reaction to the current error, integral mode determines the reaction based recent error. The weighted sum of the two mode output as corrective action for the control element. The PI controller is widely used in the industry due to its ease in design and simple structure. The PI controller algorithm can be implemented as

$$output(t) = K_p e(t) + K_i \int_0^t e(\tau) d\tau$$

Here the input to speed controller is the speed error. The output of the controller is considered as a reference torque. A limit is put on the speed controller output depending on permissible maximum winding currents.

X. MATLAB/SIMULATION RESULTS

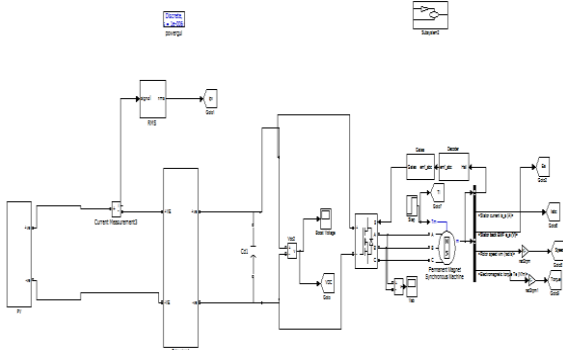
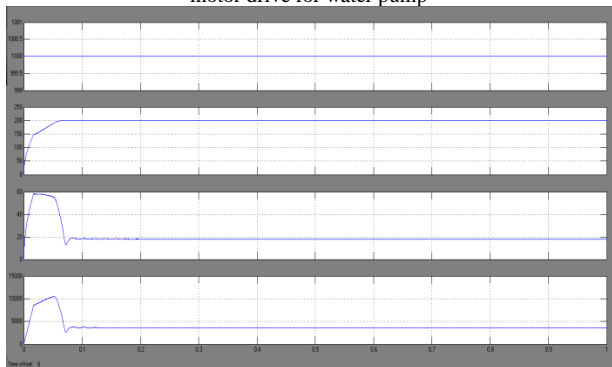
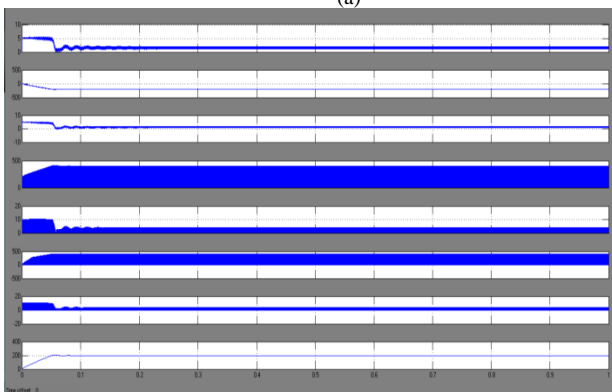


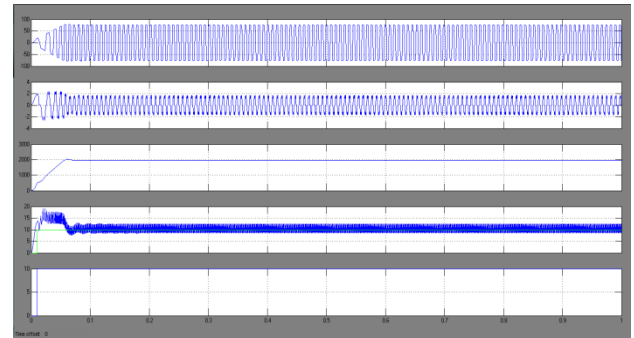
Fig. 11 Matlab/Simulink circuit of Starting and steady-state performances of the proposed SPV array based zeta converter-fed BLDC motor drive for water pump



(a)



(b)



(c)

Fig.12 Starting and steady-state performances of the proposed SPV array based zeta converter-fed BLDC motor drive for water pump. (a) SPV array variables. (b) Zeta converter variables. (c) BLDC motor-pump variables.

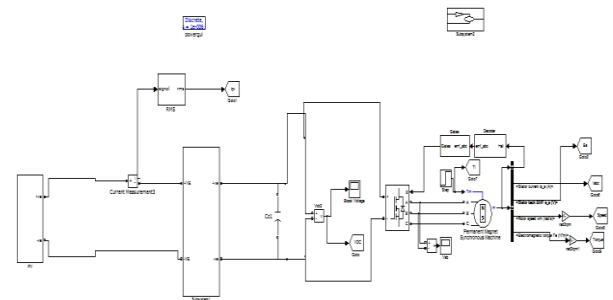
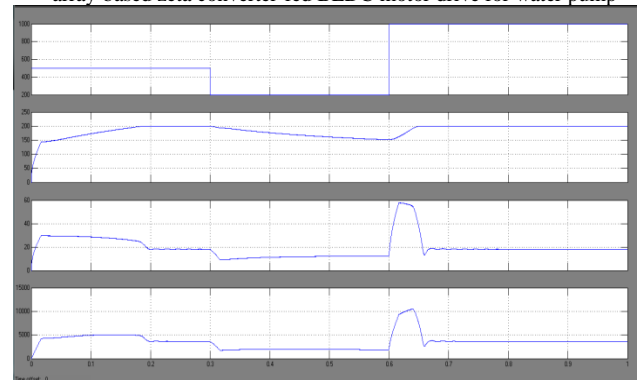
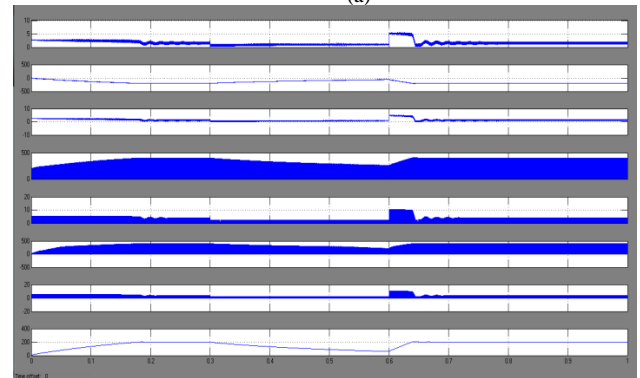


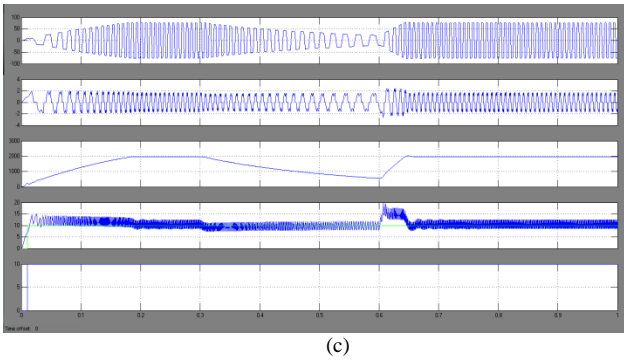
Fig.13 Matlab/Simulink circuit for Dynamic performance of SPV array-based zeta converter-fed BLDC motor drive for water pump



(a)



(b)



(c)
 Fig.14 Dynamic performances of the proposed SPV array-based zeta converter-fed BLDC motor drive for water pump. (a) SPV array variables. (b) Zeta converter variables. (c) BLDC motor-pump variables.

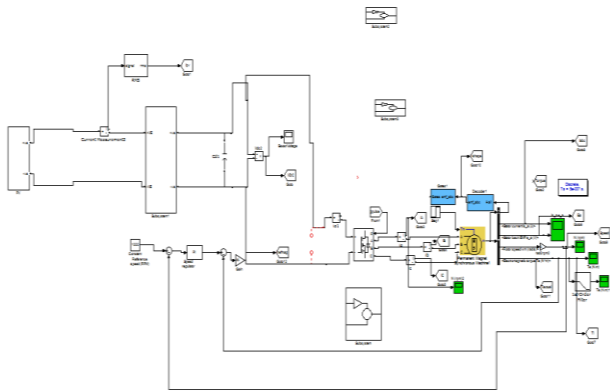


Fig.15 Matlab/Simulink circuit of SPV array-based zeta converter-fed BLDC motor drive Closed loop control for water pumping system.

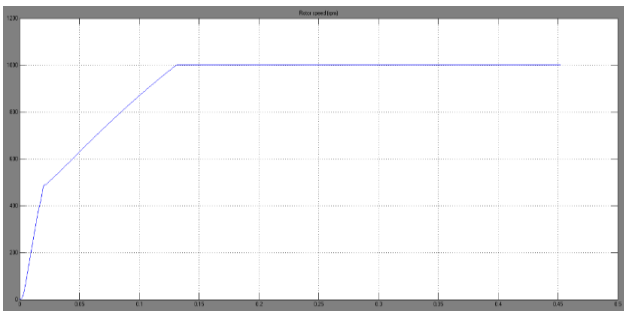


Fig.16. Speed.

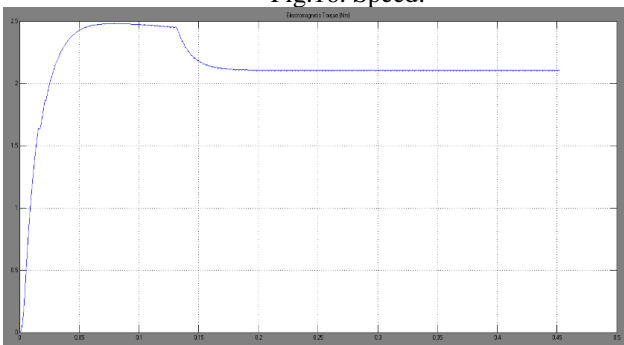


Fig.17. Torque.

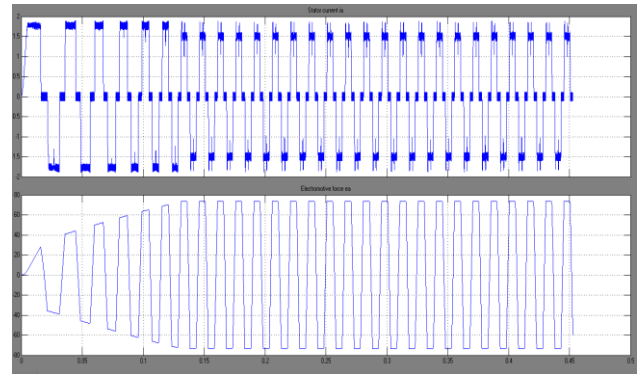


Fig.18. Stator current and emf.

XI. CONCLUSION

A solar photovoltaic array fed Zeta converter based BLDC motor has been proposed to drive water-pumping system. The proposed system has been designed, modeled and simulated using MATLAB along with its Simulink and simpower system toolboxes. Simulated results have demonstrated the suitability of proposed water pumping system. SPV array has been properly sized such that system performance is not influenced by the variation in atmospheric conditions and the associated losses and maximum switch utilization of Zeta converter is achieved. Zeta converter has been operated in CCM in order to reduce the stress on power devices. Operating the VSI in conduction mode with fundamental frequency switching eliminates the losses caused by high frequency switching operation. Stable operations of motor-pump system and safe starting of BLDC motor are other important features of the proposed system.

REFERENCES

- [1] M. Uno and A. Kukita, "Single-switch voltage equalizer using multistacked buck-boost converters for partially-shaded photovoltaic modules" IEEE Trans. Power Electron., vol. 30, no. 6, pp. 3091-3105, Jun.2015.
- [2] R. Arulmurugan and N. Suthanthiravanitha, "Model and design of a fuzzy-based Hopfield NN tracking controller for standalone PV applications," Elect. Power Syst. Res., vol. 120, pp. 184-193, Mar. 2015.
- [3] S. Satapathy, K. M. Dash, and B. C. Babu, "Variable step size MPPT algorithm for photo voltaic array using zeta converter—A comparative analysis," in Proc. Students Conf. Eng. Syst. (SCES), Apr. 12-14, 2013, pp. 1-6.
- [4] R. Kumar and B. Singh, "BLDC motor driven solar PV array fed water pumping system employing zeta converter," in Proc. 6th IEEE India Int.Conf. Power Electron. (IICPE), Dec. 8-10, 2014, pp. 1-6.
- [5] B. Singh, V. Bist, A. Chandra, and K. Al-Haddad, "Power factor correction in bridgeless-Luo converter-fed BLDC motor drive," IEEE Trans. Ind. Appl., vol. 51, no. 2, pp. 1179-1188, Mar./Apr. 2015.
- [6] B. Singh and V. Bist, "Power quality improvements in a zeta converter for brushless dc motor drives," IET Sci. Meas. Technol., vol. 9, no. 3, pp. 351-361, May 2015.
- [7] R. F. Coelho, W. M. dos Santos, and D. C. Martins, "Influence of power converters on PV maximum power point tracking efficiency," in Proc. 10th IEEE/IAS Int. Conf. Ind. Appl. (INDUSCON), Nov. 5-7, 2012, pp. 1-8.
- [8] M. A. Elgendy, B. Zahawi, and D. J. Atkinson, "Assessment of the incremental conductance maximum power point

- tracking algorithm,"IEEETrans. Sustain. Energy, vol. 4, no. 1, pp. 108–117, Jan. 2013.
- [9] M. Sitbon, S. Schacham, and A. Kuperman, "Disturbance observer based voltage regulation of current-mode-boost-converter-interfaced photovoltaic generator,"IEEE Trans. Ind. Electron., vol. 62, no. 9, pp. 5776–5785, Sep. 2015.
- [10] R. Kumar and B. Singh, "Buck–boost converter fed BLDC motor drive for solar PV array based water pumping," inProc. IEEE Int. Conf. Power Electron. Drives Energy Syst. (PEDES), Dec. 16–19, 2014, pp. 1–6.
- [11] A. H. El Khateb, N. Abd. Rahim, J. Selvaraj, and B. W. Williams, "DC to Dc converter with low input current ripple for maximum photovoltaic power extraction,"IEEE Trans. Ind. Electron., vol. 62, no. 4, pp. 2246–2256, Apr. 2015.
- [12] D. D. C. Lu and Q. N. Nguyen, "A photovoltaic panel emulator using a buck–boost dc/dc converter and a low cost micro-controller," Solar Energy, vol. 86, no. 5, pp. 1477–1484, May 2012.
- [13] Z. Xuesong, S. Daichun, M. Youjie, and C. Deshu, "The simulation and design for MPPT of PV system based on incremental conductance method," in Proc. WASE Int. Conf. Inf. Eng. (ICIE), Aug. 14–15, 2010, vol. 2, pp. 314–317.
- [14] A. R. Reisi, M. H. Moradi, and S. Jamasb, "Classification and comparison f maximum power point tracking techniques for photovoltaic system: A review," Renew. Sustain. Energy Rev., vol. 19, pp. 433–443, Mar. 2013.
- [15] B. Bendib, H. Belmili, and F. Krim, "A survey of the most used MPPT methods: Conventional and advanced algorithms applied for photovoltaic systems,"Renew. Sustain. Energy Rev., vol. 45, pp. 637–648, May 2015.



Ragolu Durgaprasad was born in srikakulam, India in 1992. He received the B.Tech. degree in Electrical and Electronics Engineering from Aditya Institute of Technology and Management, Srikakulam, India in 2013, and pursuing M.Tech. in Power electronics and Electrical Drives in

Aditya Institute of Technology and Management, Srikakulam, India.



P Guruvulunaidu received B.Tech. Degree in Electrical and Electronics Engineering from JNTU Hyderabad, India in 2006 and M.Tech. degree in Electrical Engineering from JNTU Ananthapur, India in 2008. He is pursuing Ph.D. degree in Electrical Engineering in JNTU Kakinada, India.

Currently he is working as Senior Assistant Professor in Aditya Institute of Technology and Management, Srikakulam, India.



Ch Prasad received B.E. degree in Electrical and Electronics Engineering from AU, Visakhapatnam, India in 2009 and M.E degree in Electrical Engineering from AU Visakhapatnam, India. Currently he is working as Assistant Professor in Aditya Institute of Technology and Management, Srikakulam, India.